PCCP

PAPER

View Article Online
View Journal | View Issue

Cite this: *Phys. Chem. Chem. Phys.*, 2015, **17**, 11234

Er^{3+}/Yb^{3+} upconverters for InGaP solar cells under concentrated broadband illumination

J. Feenstra,*[ab] I. F. Six,[a] M. A. H. Asselbergs,[a] R. H. van Leest,[a] J. de Wild,[c] A. Meijerink,[d] R. E. I. Schropp,[ef] A. E. Rowan[b] and J. J. Schermer[a]

Received 21st August 2014,
Accepted 8th October 2014

DOI: 10.1039/c4cp03752a

www.rsc.org/pccp

The inability of solar cell materials to convert all incident photon energy into electrical current, provides a fundamental limit to the solar cell efficiency; the so called Shockley–Queisser (SQ) limit. A process termed upconversion provides a pathway to convert otherwise unabsorbed low energy photons passing through the solar cell into higher energy photons, which subsequently can be redirected back to the solar cell. The combination of a semi-transparent InGaP solar cell with lanthanide upconverters, consisting of ytterbium and erbium ions doped in three different host materials (Gd_2O_2S, Y_2O_3 and $NaYF_4$) is investigated. Using sub-band gap light of wavelength range 890 nm to 1045 nm with a total accumulated power density of 2.7 kW m^{-2}, a distinct photocurrent was measured in the solar cell when the upconverters were applied whereas a zero current was measured without upconverter. Furthermore, a time delay between excitation and emission was observed for all upconverter systems which can be explained by energy transfer upconversion. Also, a quadratic dependence on the illumination intensity was observed for the $NaYF_4$ and Y_2O_3 host material upconverters. The Gd_2O_2S host material upconverter deviated from the quadratic illumination intensity dependence towards linear behaviour, which can be attributed to saturation effects occurring at higher illumination power densities.

Introduction

In photovoltaics, only photons with energies equal to or greater than the band gap are commonly used to generate electric current. The inability of solar cell materials to convert all incident photon energy into electrical current, provides a fundamental limit to the solar cell efficiency; the so called Shockley–Queisser (SQ) limit.[1] The main loss processes are thermal losses from excess photon energy and transmission losses of photons with energies lower than the band gap. A process termed upconversion provides a pathway to convert otherwise unabsorbed low energy photons passing through the solar cell into higher energy photons,[2,3] that subsequently can be redirected back to the solar cell.

Among various possible upconversion systems[3–5] lanthanide-doped materials are of particular interest.[5–13] Lanthanides are the elements 57 (La) to 71 (Lu) in the periodic table for which the 4f inner shell is being filled up to 14 electrons. Lanthanides usually occur in their trivalent form (Ln^{3+}) in which they have n electrons in the 4f shell, providing $\binom{14}{n}$ possible electron configurations, each with a different energy level. Changing the host material into which the lanthanides are dispersed provides a certain control over the absorption and emission behaviour of the lanthanide ions. For the present study upconverters based on the Er^{3+}/Yb^{3+} lanthanide pair will be used.[14]

In previous studies the performance of these upconverters in combination with amorphous silicon solar cells was evaluated[15] but the sub-band gap absorption of a-Si overlaps with the active absorption bands of the lanthanides.[14,16] It is suggested in literature[17] to use GaAs solar cells because their absorption range, with a band gap cut-off wavelength of about 875 nm, is just outside the absorption range of the lanthanides. However, preliminary experiments for the present study showed that, although it is very small, the sub-band gap absorption of semi-transparent GaAs solar cells also overlaps with the absorption range of the used Er^{3+}/Yb^{3+} upconverters. Other type III–V solar cells such as InGaP cells have a band gap cut-off at lower wavelengths (700 nm for $E_g = 1.8$ eV). Therefore, in this work the use of upconverters is studied in combination with a thin-film semi-transparent InGaP solar cell as obtained by the Epitaxial-Lift-Off process.[18] In particular a comparative study of upconverter

[a] *Applied Materials Science Department, Radboud University, Nijmegen, The Netherlands. E-mail: j.feenstra@science.ru.nl*
[b] *Molecular Materials Department, Radboud University, Nijmegen, The Netherlands*
[c] *Condensed Matter and Interfaces Department, Utrecht University, Utrecht, The Netherlands*
[d] *Gabriel Lippmann Institute, Luxembourg University, Luxembourg, Luxembourg*
[e] *Energy Research Centre of the Netherlands (ECN), Solar Energy, High Tech Campus Eindhoven, The Netherlands*
[f] *Department of Applied Physics, Plasma & Materials Processing, Eindhoven University of Technology (TU/e), Eindhoven, The Netherlands*

behaviour influenced by fluoride ($NaYF_4$), oxide (Y_2O_3) and oxysulfide (Gd_2O_2S) host materials is provided.[3,19,20]

For a two-photon upconversion process, emission intensity is known to scale quadratically with the illumination intensity since two photons are required within the excitation lifetime of the lanthanide ion responsible for absorption of photons (Yb^{3+}).[17,21] The additionally obtained photocurrent will therefore also scale quadratically with the illumination. This suggests that the best opportunities, for use of lanthanide upconverters in combination with solar cells, might be in concentrated light applications with a high concentration ratio. Such concentrated photovoltaic (CPV) systems generally are also equipped with type III–V solar cells.

At variance with most research on the subject of enhancing solar cell performance using lanthanide upconverters,[3,4,9,16,18,20–27] the current study focuses on the use of broadband illumination utilizing a flash light set-up instead of laser excitation at specific wavelengths. This is done to more closely approach the conditions under which the system should perform in any practical application.

Theory

Upconversion

The energy level structure of the Er^{3+}/Yb^{3+} ion upconverter is schematically depicted in Fig. 1. The partially filled 4f shell provides the unique optical and magnetical properties of lanthanides. The 4f orbitals are shielded from the surroundings by the filled $5s^2$ and $5p^6$ orbitals. Therefore the influence of the host lattice on the optical transitions in the $4f^n$ configuration is relatively small, but essential to the upconversion process.[28]

Theoretically, the 4f → 4f transitions are not allowed under the Laporte rule, stating that transitions involving symmetrical orbitals are parity forbidden. However, small changes in symmetry of the orbital configuration, due to admixture of opposite parity states, which are induced by odd-parity crystal field components, provide deviation from the symmetry which makes the transfer slightly allowed. The host material influences the transitions in the 4f shells. For increasing covalence of the host materials the electronic transitions between energy levels with an energy difference, which is determined by electron interaction, shift to lower energy.[28] A higher covalence, as in oxysulfide or oxide host materials, makes the transition more allowed in comparison to fluoride host materials leading to a broader and stronger absorption band.

Following the absorption, energy transfer between the 4f shells of two lanthanide ions can occur *via* resonance of their dipole moments, consistent with the energy transfer upconversion (ETU) process it uses. This occurs if two conditions are met. Firstly, the spectral overlap between emission of the Yb^{3+} and the absorption of the Er^{3+} should be sufficient and secondly, the two ions should be in close proximity to each other. The latter can be obtained by high doping concentrations, which for lanthanide upconverters might be up to 20%.[3] However, a material specific limit to doping must be taken into consideration to prevent quenching effects. The first condition can be influenced by the phonon energy of the host material. Although low, the phonon energy of the host lattice can aid the transition between two ions if their excited state levels are slightly unmatched.

For the particular upconverters evaluated in this study consisting of Er^{3+}/Yb^{3+} ions doped in host materials of fluoride ($NaYF_4$), oxide (Y_2O_3) or oxysulfide (Gd_2O_2S), the upconversion principle (see Fig. 1) works as follows. The absorption of energy takes place by excitation of the, so called, sensitizer (Yb^{3+}) from the $^2F_{7/2}$ to the $^2F_{5/2}$ energy level. After absorption, the energy is transferred by the sensitizer returning from the excited state ($^2F_{5/2}$) to its ground state while simultaneously the Er^{3+} ion, in this role referred to as activator, is excited to the $^4I_{11/2}$ or the $^4F_{7/2}$

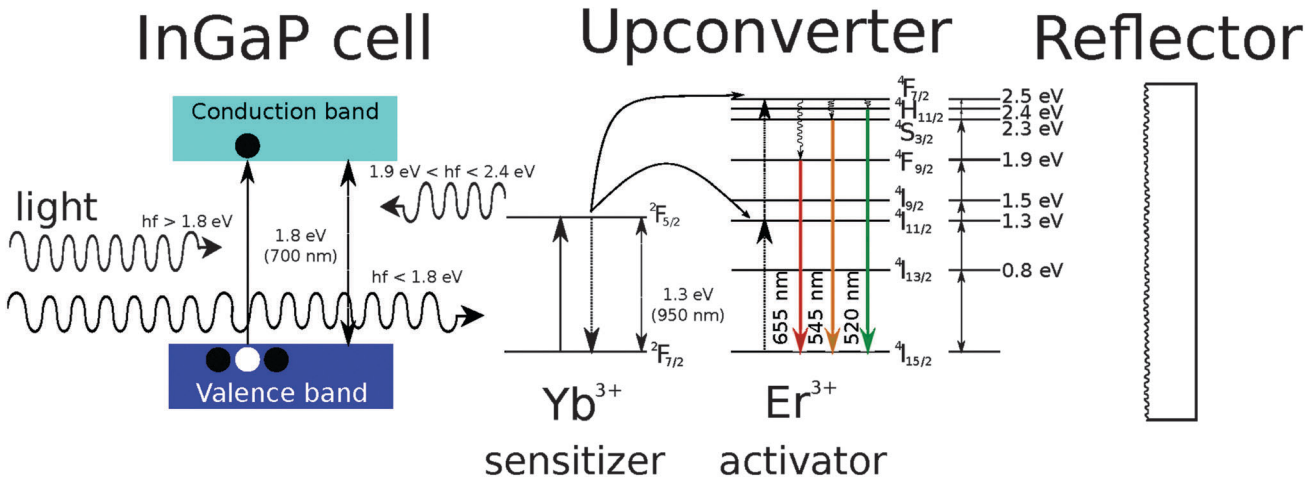

Fig. 1 The UpConverter-System (USC) used in this study showing the principle of upconversion in host material containing the Er^{3+}/Yb^{3+} system in combination with an InGaP solar cell. The figure shows photovoltaic conversion in the InGaP solar cell utilizing photons with energies exceeding 1.8 eV (700 nm) and the upconversion of photons with energies in the 1.3 eV (950 nm) range to higher energies between 1.9 eV (655 nm) and 2.4 eV (520 nm). These photons are reflected back, using a diffuse white back reflector, into the InGaP solar cell.

energy level. The spectral overlap between the Yb^{3+} and Er^{3+} ions is sufficient and doping concentrations in various host materials are high enough for ETU.

Due to shielding of the 4f orbital, the electron–phonon coupling strength is low. The parity is unchanged in the electron transition to the ground state and therefore the lifetime of the excited state is relatively long (up to 10^{-3} s).[28] The optimal level of phonon interaction from the host material should induce relaxation from the $^4F_{7/2}$ excited state to the lower intermediate states $^2H_{11/2}$, $^4S_{3/2}$ and $^4F_{9/2}$[14] while extended multi-phonon relaxation to the ground state is prevented. Subsequently radiative decay from the intermediate energy levels to a lower lying state is possible resulting in several emission bands (see the right hand side of Fig. 1).

Upconversion efficiency

In applications the lanthanide doped host materials are dispersed in a poly(methyl methacrylate) (PMMA) layer. This assembly will be referred to as upconverter system (UCS) and from here on upconverter-host materials will be indicated with the name of the host material followed with UCS. The UCS is placed behind a semi-transparent solar cell so that photons unabsorbed by the cell are collected by the upconverter. Here two lower energy photons can be converted into one higher energy photon, which is emitted back towards the solar cell utilizing a diffuse white reflecting layer at the bottom of the UCS. The power gain in the solar cell due to the upconverted photons is dependent on the solar cell's photovoltaic conversion efficiency in the wavelength region of the upconverter emission under rear side illumination.[2,29]

A variety of definitions is used to describe the efficiency of the upconversion process. Frequently the quantum efficiency is defined by comparing the emitted energy of the lanthanides ions with the energy they effectively absorb. For the upconversion of 980 nm to 540 nm photons in Er^{3+}/Yb^{3+} systems, typical upconversion quantum efficiencies are 5.5% for 200 kW m^{-2} up to 10% for 400 kW m^{-2}.[3] Alternatively, the number of photons emitted is compared to the number of absorbed photons. With this definition the upconversion efficiency can maximally be 50%. However, for use in PV applications it is more important to relate the upconverted short wavelength photon energy emitted by the whole UCS to the irradiated long wavelength photon energy. In this way one also takes into account the non-perfect absorption of the lanthanide ions and other parasitic absorption losses in the host material or supporting PMMA layer. In the present study we will take this one step further towards the use in PV systems and define the PV UpConversion System Efficiency (PVUCS-E) as the ratio between the obtained photocurrent in the solar cell from upconverted photons over the current generated in the bare solar cell (*i.e.* without UCS but with back reflector) illuminated with the AM1.5 standard spectrum at the appropriate concentration ratio.

The absorbed power density of a UCS under standard standard test conditions (STC) is given by:

$$P_{uc,STC} = \int P_{STC}(\lambda) A_{uc}(\lambda)\, d\lambda \quad (1)$$

In which, $P_{STC}(\lambda)$ is the AM1.5 spectral distribution with a total intensity of 1000 W m^{-2} and A_{uc} the absorption in the UCS. In a similar way the absorbed power density of the UCS under standard flash light illumination is given by:

$$P_{uc,flash} = \int P_{flash}(\lambda) A_{uc}(\lambda)\, d\lambda \quad (2)$$

In which $P_{flash}(\lambda)$ is the spectral distribution at the maximum power density during the flash. The maximum AM1.5 based concentration ratio experienced by the UCS under flash light illumination during the experiments is given by:

$$C_{uc} = \frac{P_{uc,flash}}{P_{uc,STC}} \quad (3)$$

We will refer to this quantity as the upconverter absorbed concentration factor. For practical applications this would be the concentration ratio required by the PV-UCS combination to generate the reported additional short-circuit current densities ($J_{sc,uc}$) in this study. For single-junction type III–V solar cells under moderate concentration ratios up to about 50 suns the short-circuit current can be taken to be proportional to the illumination density. As we do not use C_{uc} in excess of 50 suns the current density of the bare cell under the above determined concentration ratio is given by:

$$J_{sc,cell} = C_{uc} J_{sc,STC} \quad (4)$$

with $J_{sc,STC}$ the short circuit current density of the bare cell under standard test conditions (AM1.5, 1000 W m^{-2} and 25 °C). Subsequently the PV UpConversion System Efficiency (PVUCS-E) is given by:

$$\text{PVUCS-E} = \frac{J_{sc,uc}}{J_{sc,cell}} \quad (5)$$

Experimental

In this study four different upconverter-host combinations were studied. The first two were 1% Er^{3+}/9% Yb^{3+} and 1% Er^{3+}/18% Yb^{3+} both in $NaYF_4$ host material, synthesized at the department of Condensed Matter and Interfaces at Utrecht University. The other two were commercially available Er^{3+}/Yb^{3+} upconverters in Y_2O_3 and Gd_2O_2S hosts, obtained from Phosphor Technology. Previous studies[14] indicated the Er^{3+} and Yb^{3+} concentrations, in both systems, to be 5% and 10% respectively. Each upconverter was provided in powder form and was added to a mixture of PMMA in chloroform with a volume ratio 1 : 10. This was deposited on a white diffusive reflecting tape[8,14] on top of a glass plate and dried for 4 hours to form a solid layer. The reflective tape was developed by DuPont and Oerlikon Solar[8] and has a reflectance of more than 95% independent of wavelength.[14]

The thus obtained UCS were used together with a 1.0 × 2.0 cm^2 semi-transparent InGaP solar cell. The InGaP structure was grown by low pressure metal organic vapour phase epitaxy (MOVPE) on a 2 inch diameter (100) GaAs wafer with a misorientation of 2° towards [110]. To obtain a thin-film semi-transparent cell, an AlAs release layer with a thickness

of 10 nm was grown first, followed by the layers of the 1 μm thick InGaP cell structure. Using Epitaxial Lift-Off, the layers on top of the AlAs layer were separated from their original substrate by etching of the sacrificial AlAs layer with 10% aqueous HF. This results in a thin-film layer stack on a foreign plastic carrier. Further thin-film solar cell processing involves transfer to a rigid glass carrier, electron-beam evaporation of gold alloyed aligned grid contacts at both sides to obtain maximum transmission of unabsorbed photons and mesa etching.[18,31] The coverage of the grid patterns was 7% of the solar cell on the front-side and (resulting from a larger contact area) 8% on the back-side. The cell was not coated with an anti-reflection coating.

Before integration with UC-systems, the performance of the bare InGaP cells were determined under front side illumination (FSI) as well as back side illumination (BSI). The *I–V* characteristics of the cells under the 1000 W m^{-2} AM1.5 standard solar spectrum were determined using a solar simulator (ABET Sun 2000) connected to a Keitley 2600 voltmeter and Tracer2 software (ReRa Solutions®). Before measurement the light intensity is set using a GaAs reference cell, which was calibrated at the National Renewable Energy Laboratory (NREL). The back side illumination external quantum efficiency (EQE) was measured by a ReRa Solutions SpeQuest system with an Omni 150 monochromator and a Hg-lamp. Calibration was performed using a ThorLabs Si photodiode with known spectral response and a systematic error smaller than 3%. During FSI measurements a white reflective background was used in order to make comparison of cell performance with and without UCS justified.

Fig. 2 shows a schematic drawing of the setup used for the measurement of the solar cell photocurrent resulting from upconversion. The measurement of the spectral irradiance, absorption and emission of the upconverter in absence of the solar cell were also performed in this setup. A xenon flash lamp is used as broadband light source. This lamp gives pulses of approximately 4 ms of light with intensity up to several hundred suns at the sample distance used in this study. The InGaP cell and the UCS are placed in a box below the flash lamp. The interior of this measurement box has a non-reflective black surface. Light from the lamp can only enter the box through an opening straight below the lamp. For measurement of response to sub-band gap light all light of wavelengths below 900 nm is blocked by a longpass filter. InGaP has a band gap of 1.88 eV (corresponding to a cut-off wavelength of 660 nm), which means that the longpass filtering removes all light that could be photovoltaically converted during the first pass of light.

The setup contains a beam splitter, which deflects a fraction of approximately 8% of the incoming light to a photodiode and transmits the remaining light towards the solar cell and/or UCS.

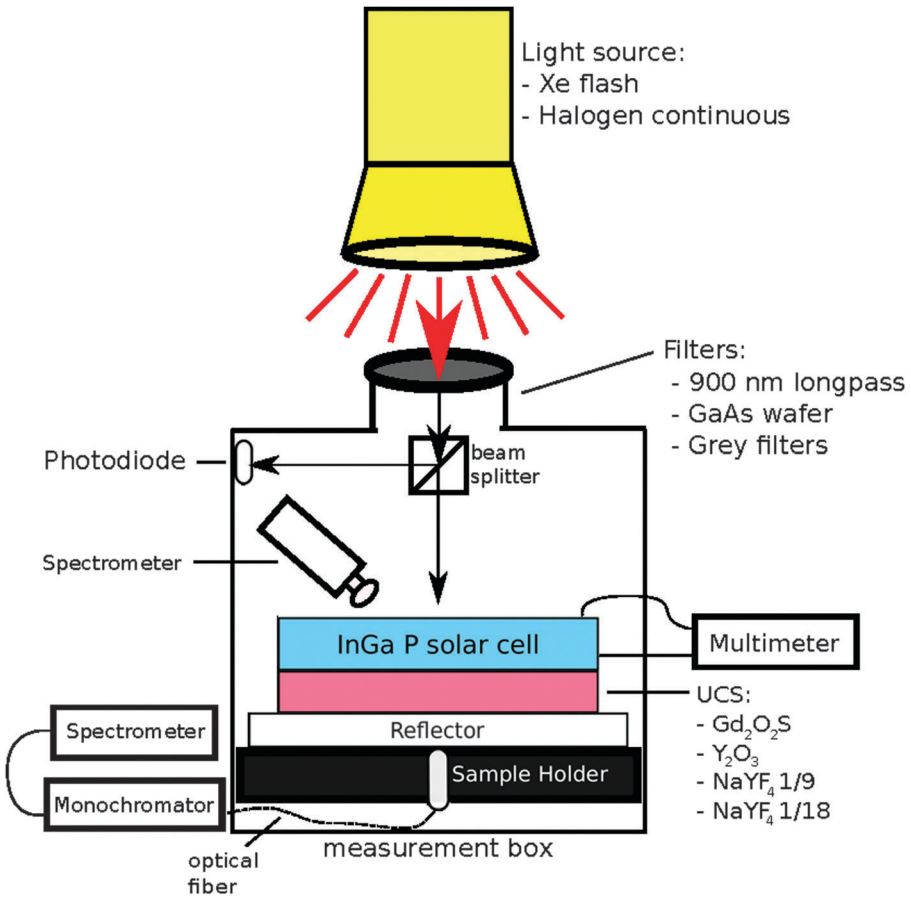

Fig. 2 Schematic overview of the setup for measurement of upconverters performance. Showing the measurement box with exchangeable light sources, filters, UCS, several recording devices and optional position of the solar cell.

Using a large range photocurrent amplifier both the current of the photodiode and the short circuit current density of the solar cell could be measured simultaneously as a function of time during the Xe light flashes. On forehand the photodiode signal was related to the power density of the light source on the PV cell in a separate calibration procedure.

The power of the illumination on the PV cell was varied by placing different additional grey filters in the opening of the measurement box. Twelve different grey filters were used, having transmissions between 1% and 98% relatively independent of the wavelength. Following this procedure, the dependence of the solar cell current on the illumination power was obtained for all upconverter systems.

In a similar way as described in a previous study[14] the absorption spectra of the upconverter systems were derived from reflection measurements. For these measurements the filters were removed from the opening of the measurement box and the Xe flash lamp was replaced with a continuous halogen light source. The diffusely reflected light was recorded using an Ocean Optics USB4000 Fibre Optic Spectrometer, whose operation is based on a linear CCD array. The reflection of a reference sample, consisting of Oerlikon white reflective foil without upconverter, was measured as well. The emission spectra were obtained in a similar way but with the 900 nm longpass filter placed in the opening of the box to ensure that only upconverted sub-900 nm light was detected.

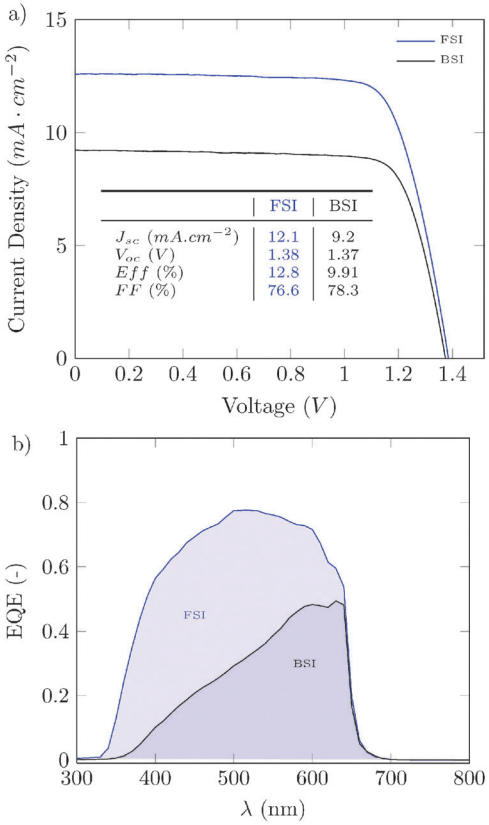

Fig. 3 J–V (a) and external quantum efficiency (b) of a 1.0 × 2.0 cm^2 bifacial ELO InGaP solar cell with a thickness of 1.0 μm for both front side illumination (FSI) and back side illumination (BSI).

Results

Semi-transparent InGaP solar cell

Fig. 3 shows the J–V and quantum efficiency of the semi-transparent InGaP cell used in the present study under front side illumination (FSI) and back side illumination (BSI). The layer structure of the InGaP solar cell was previously developed for operation with a regular full back contact. Fig. 3 indicates that modification of the cell structure to optimize the cell performance under back side illumination would be beneficial to maximize the upconverter induced photocurrent. However, optimization of the cell current for back-side illumination will come at the cost of its performance under front side illumination and in fact would only be justified if upon modification the total cell-UCS would perform better than the present bare cell. Even if an efficiency gain of 1% under BSI comes at a loss of only 0.1% under FSI, this would only be justified if the PVUCE would be in range of 0.1%. As will be shown later in this study, this is not the case in the present stage of research.

Absorption and emission of the upconverter systems

The absorption spectra of the studied upconverter systems are shown in Fig. 4. All UCS show a broad absorption band ranging from 900 nm to slightly more than 1000 nm, which is attributed to both the Yb^{3+}: $^2F_{7/2} \rightarrow {}^2F_{5/2}$ transition and the Er^{3+}: $^4I_{15/2} \rightarrow {}^4I_{11/2}$ transition. The other absorption peaks are all attributed to Er^{3+} transitions. The position of the absorption features in the spectra is quite similar but their magnitude and shape differ depending on the host material. For the oxysulfide UCS the sensitizers absorption band is significantly larger than for the other three host materials because the energy transitions associated with the absorption are more allowed through the interaction of the sensitizer with the more covalent oxysulfide host.

Comparison of the absorption spectra with the flash light spectra and AM1.5 spectra, in the wavelength range above the cut-off wavelength of the solar cell, gives an indication of the fraction of incident light that can be absorbed by the upconverter when used under flash light and in the field. Fig. 5 shows the overlap between the absorption bands of the sensitizer and the AM1.5 spectrum. Upconverter absorbed power ($P_{uc,flash}$ and $P_{uc,STC}$) values for the different upconverters as calculated using eqn (1) and (2) are shown in Table 1.

Fig. 5 shows that the sensitizer absorption band of the Gd_2O_2S UCS coincides with a low irradiance part known as a "water hole" in the AM1.5 spectrum. Nevertheless, even under the AM1.5 spectrum, the absorption in the oxysulfide host material UCS is still higher than of the other UCS investigated in this study.

Under broadband illumination ranging from 900 nm to 1050 nm each of the four UCS show emission with multiple peaks around 545 nm and 680 nm. The overlap between the emission bands of the upconverters and the QE of the InGaP cell under rear side illumination is shown in Fig. 6. The Y_2O_3

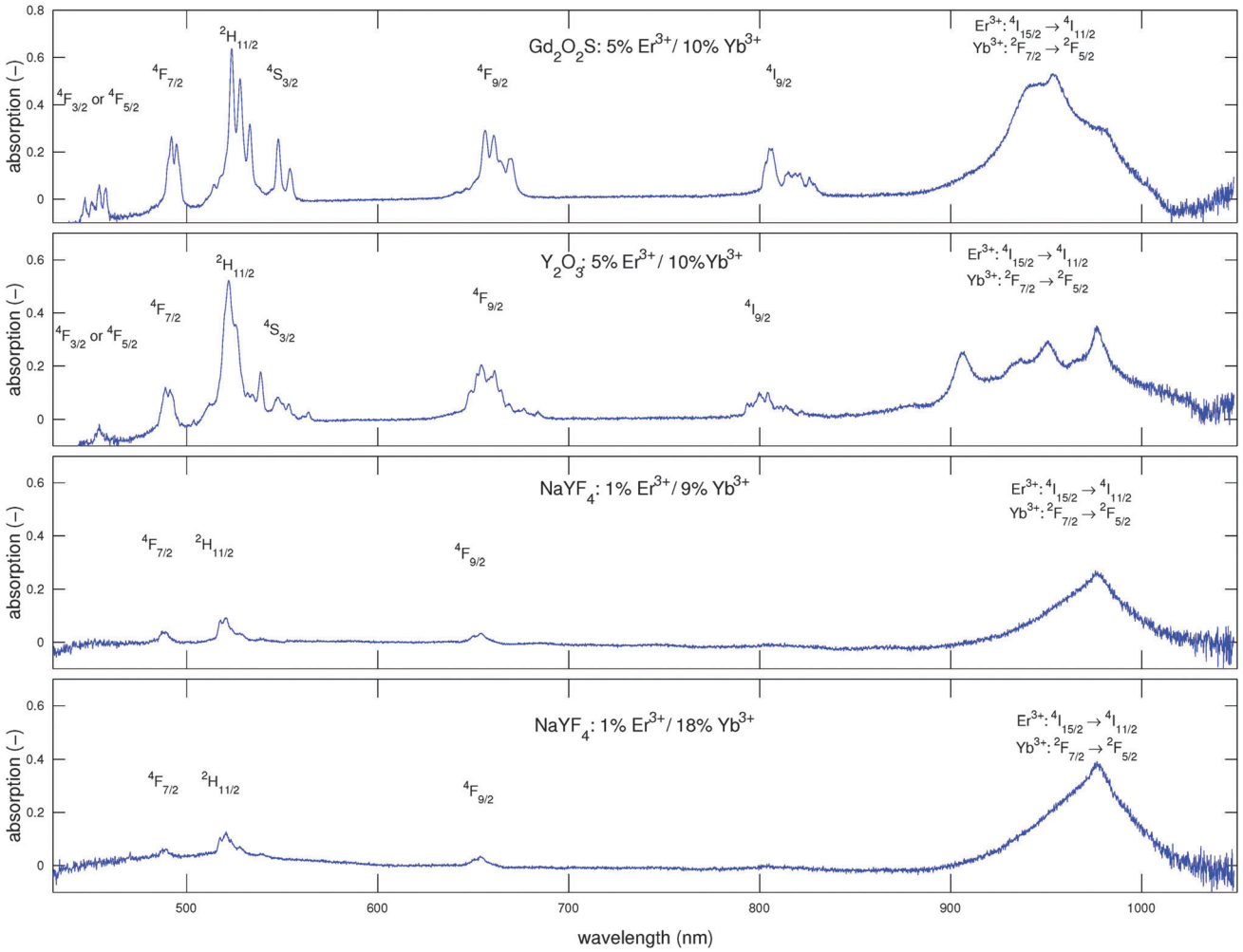

Fig. 4 The absorption spectra of Er^{3+}/Yb^{3+} upconverters in $NaYF_4$, Y_2O_3 and Gd_2O_2S host materials. The peaks are annotated with the excited state with which they correspond.

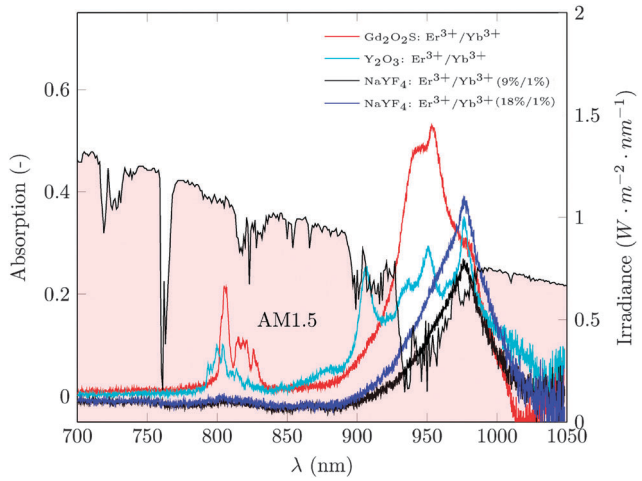

Fig. 5 The overlap between the relevant absorption bands of the four upconverter types used in this study (left axis) and the power density distribution of the AM1.5 standard spectrum (black line with red fill, on the right axis).

Table 1 Overview of several upconverters showing: the upconverters absorbed power densities from the flash light ($P_{uc,flash}$) and the standard test conditions ($P_{uc,STC}$), the maximum AM1.5 based concentration factor experienced during flash illumination (C_{uc}), the maximum current density ($max(J_{sc,uc})$), the PV-UCS Efficiency (PVUCS-E) and the time delay (Δt) between the maximum intensity of the flash and the maximum current density in the PV cell

Upconverter (host: Er^{3+}/Yb^{3+})	$P_{uc,flash}$ (W m^{-2})	$P_{uc,STC}$ (W m^{-2})	C_{uc} (–)	$max(J_{sc,uc})$ (mA cm^{-2})	PVUCS-E (%)	Δt (ms)
Gd_2O_2S: 5%/10%	595	12.8	47	0.10	17.6×10^{-3}	0.6
Y_2O_3: 5%/10%	422	11.7	36	3.9×10^{-3}	0.90×10^{-3}	1.6
$NaYF_4$ 1%/9%	284	7.5	38	4.0×10^{-3}	0.88×10^{-3}	1.9
$NaYF_4$: 1%/18%	415	10.8	39	3.5×10^{-3}	0.72×10^{-3}	1.4

UCS emits most of its light outside the functional wavelength range of the InGaP cell, mainly due to the higher phonon energy of the host material which increases the possibility of multi-phonon relaxation in the activator (Er^{3+}). This upconverter type is therefore less suitable to be used in combination with an InGaP solar cell. The Gd_2O_2S UCS has a much higher emission than the other three UCS, as a result of its stronger absorption and more effective ETU. This can be observed from the order of

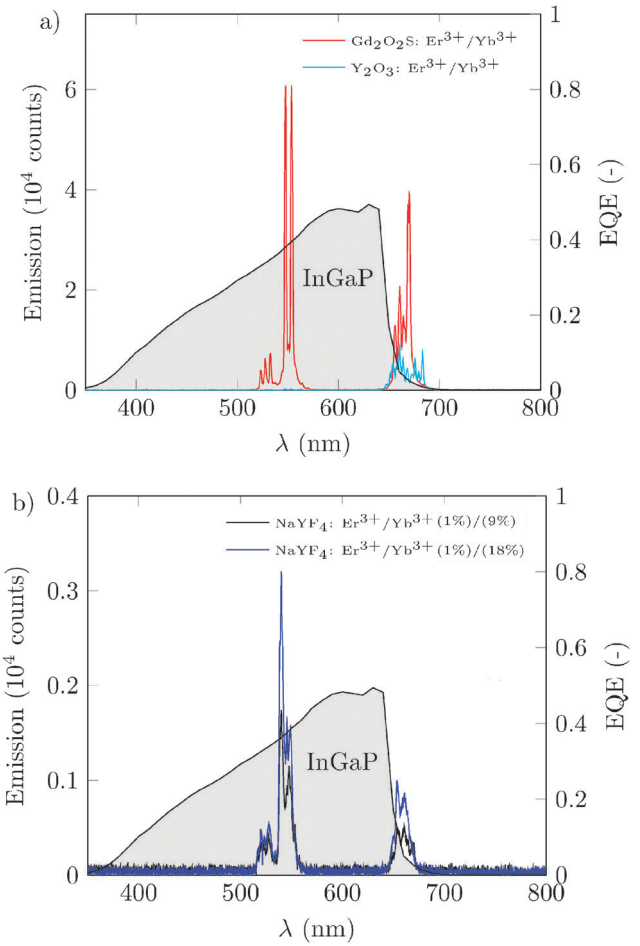

Fig. 6 Relative emission spectra of the four different upconverters (a: Gd_2O_2S and Y_2O_3 UCS; b: $NaYF_4$ UCS) as obtained with equal recording time (left axes) in relation to the quantum efficiency of the semi-transparent InGaP solar cell under back-side illumination (right axes).

magnitude larger emission indicated in Fig. 6. The difference in emission in the $NaYF_4$ with 9% or 18% Yb seems consistent with the relative difference in absorption indicated in Fig. 5. The host material has, in this particular case, the most significant influence on the upconversion process.

PV-UCS performance under 900–1050 nm flash light illumination

Fig. 7 shows the power density distribution (PDD), of the used flash lamp, over wavelength and time. The maximum power density in the investigated wavelength range of 900–1050 nm during a flash is about 2.7 kW m^{-2}. Comparing this to the power density of the "one sun" AM1.5 spectrum, which, in the same wavelength range, accumulates to 83 W m^{-2}, leads to the conclusion that in this range the flash light source delivers a light intensity equivalent to about 32 suns.

The wavelength dependency of the absorption makes comparing upconverters difficult. Therefore eqn (2) is used to integrate over the wavelength leading to an upconverter absorbed power from the flash lamp ($P_{uc,flash}$). Furthermore, the AM1.5 based upconverter absorbed concentration factor is

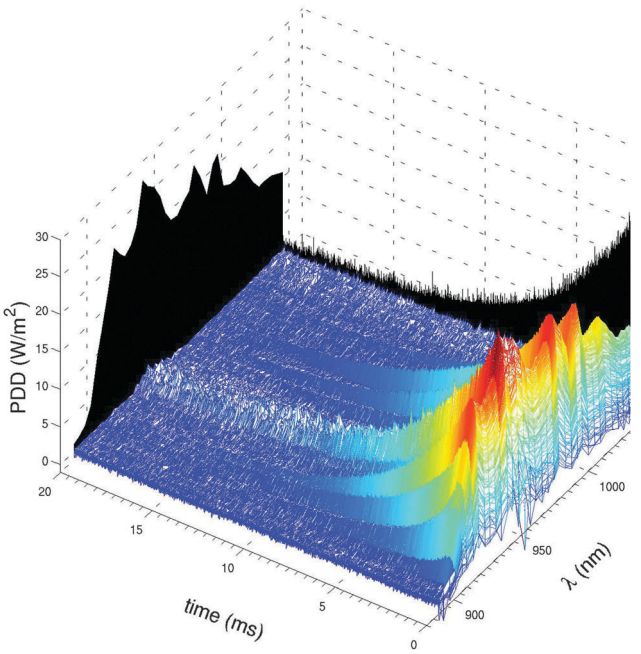

Fig. 7 Power density distribution (PDD) of the flash light as function of the wavelength and time. Projections of the maxima per wavelength and over time are displayed on the side planes.

calculated *via* eqn (4). The values of $P_{uc,flash}$, $P_{uc,STC}$ and C_{uc}, for each of the four UCS used, are stated in Table 1.

Fig. 8 shows the simultaneously recorded power density of the Xenon lamp and $J_{sc,uc}$ of the InGaP cell for each of the UCS examined in this study. The black dashed line represents the situation when no UCS is used which confirms that the recorded $J_{sc,uc}$ signal indeed solely originates from upconverted photons. The figure also shows a clear time delay between the maximum intensity of the flash and the current generated in the InGaP solar cell. The values of the time delays are stated in Table 1. To reduce noise, the measured signals were smoothed before the maxima were determined. As expected from its larger absorption and ETU, the time delay is shortest in the Gd_2O_2S UCS. Accordingly, a longer time delay in the $NaYF_4$ UCS with the lower concentration of Yb^{3+} is observed, compared to that of the higher concentration of Yb^{3+} in the same host material.[5,24]

The illumination intensity dependence of the photovoltaic current density due to upconversion was studied using a set of neutral density filters with various transmissions. For each filter, flash power density and $J_{sc,uc}$ were measured during ten flashes. Fig. 9 shows the maximum of the upconverter induced current density ($J_{sc,uc}$) in the InGaP cell as a function of the maximum power density of the flash (P_{flash}) in the wavelength range from 900 nm to 1050 nm. Each point represents the measurement during one flash and series of data collected at two or three different occasions with intervals of at least one day are independently identified.

The data of each series was fitted with an exponential function according to:

$$J_{sc,uc} = aP_{flash}^{b} \quad (6)$$

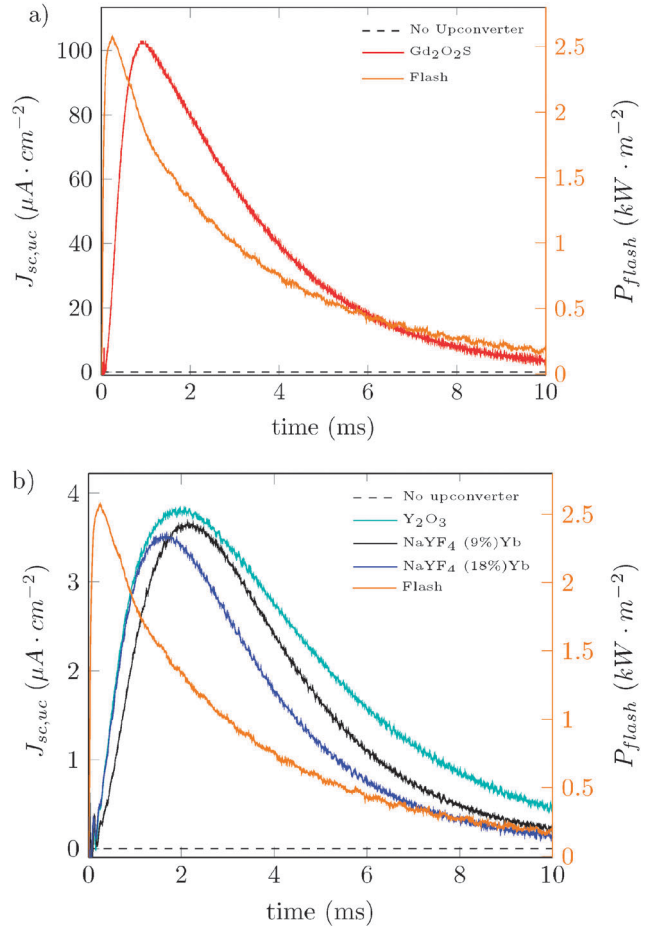

Fig. 8 Illumination power density of the flash (right-axis in orange) and the short-circuit photocurrent generated in the InGaP solar cell (left-axis) during flash using four different upconverters. (a) the Gd_2O_2S UCS (b) the Y_2O_3 and both $NaYF_4$ UCS. In both graphs the black dotted line indicates the current measurement in the InGaP solar cell without upconverter, in which case there is no photovoltaically generated current.

using the program SciDAVis, which uses a scaled Levenberg–Marquard algorithm, considered as a standard nonlinear least squares algorithm. SciDAVis provides the slope '*a*' and the exponent '*b*' with errors computed from the scatter of the data.[30] The parameters are shown in Table 2. The values of the coefficient of determination (R^2) are close to 1, indicating that the lines fit the data very well. The values of the slope '*a*' vary slightly between different series of the same upconverter, probably because of variations in the positioning of the solar cell, the upconverter or the filters in the setup. Note that the solar cell and upconverter were removed from the setup between the series. For the Gd_2O_2S UCS, the exponent '*b*' is significantly lower than 2, being the theoretically expected value for a two photon upconversion process as described earlier. A theoretical study using a rate-equation model showed that this quadratic dependence is only valid at low excitation power, when linear decay of the intermediate excited state dominates upconversion.[21] In the high power limit upconversion is dominant, and the emission is linearly proportional to the excitation power. Pollnau *et al.*[21] verified this model by several experiments. Furthermore it is also valid for energy transfer upconversion in which the sensitizer and acceptor are separate ions.[20] The decrease in the exponent '*b*' towards 1 is referred to as upconverter "saturation". For the Y_2O_3 and $NaYF_4$ UCS the measured values of '*b*' are between 1.9 and 2.0. This means that a near quadratic relationship between the illumination power density and the solar cells photocurrent was observed. For these upconverters the illumination power density was too low for saturation.

The observation that the Gd_2O_2S upconverter begins to saturate has implications for its applicability under high power densities. The power dependence of the upconverter quantum efficiency is determined by:

$$\mathrm{EQE} \propto \frac{P_{\mathrm{em}}}{P_{\mathrm{abs}}} \propto \frac{P_{\mathrm{abs}}^{b}}{P_{\mathrm{abs}}} \propto P_{\mathrm{abs}}^{(b-1)} \tag{7}$$

where P_{abs} and P_{em} are the absorbed and emitted power respectively. As long as $b > 1$, the efficiency increases as function of light power. However, if the upconverter is fully saturated, which is the case if $b = 1$, increasing the light power has no beneficial effect on the quantum efficiency of the upconverter. This implies that the potential solar cell enhancement under higher concentrations of sunlight may be larger for the Y_2O_3 and $NaYF_4$ UCS than for the Gd_2O_2S UCS.

PVUCS efficiency

The PV-UCS efficiency (PVUCS-E) was earlier defined as the relative increase of the performance of a PV cell upon the addition of an upconverter system. For the highest light concentration values encountered by the UCS in this study the PVUCS-E values are determined using eqn (5) and shown in Table 1. The Y_2O_3 and $NaYF_4$ UCS realize an additional performance of less than 10^{-3}%. The additional performance obtained by the Gd_2O_2S UCS is about 20 times higher. However, this system also provides a relative contribution of less than 0.02% to the performance of the PV cell even though the operation of this particular system already starts to move towards its saturation range. Clearly significant improvements in upconverter performance have to be realized to justify the development of dedicated semi-transparent PV cell structures to be used in combination with such systems and to further evaluate their potential in actual CPV systems. For the current research it will be sufficient just to replace the full back contact of a regular thin-film III–V solar cell by a grid contact in the experimental investigation of upconverter systems.

Discussion & conclusion

In this study, the combination of an InGaP solar cell with Er^{3+}/Yb^{3+} upconverters was investigated. Four upconverter systems with different host materials and lanthanide concentrations were studied: Gd_2O_2S and Y_2O_3 both with 5% Er^{3+}/10% Yb^{3+} concentrations and $NaYF_4$ with 1% Er^{3+}/9% Yb^{3+} and 1% Er^{3+}/18% Yb^{3+}. All UCS show a broad absorption ranging from 900 nm to 1000 nm, and emission around 550 nm and around 660 nm. The Gd_2O_2S UCS is the strongest absorber. However, the maximum of the

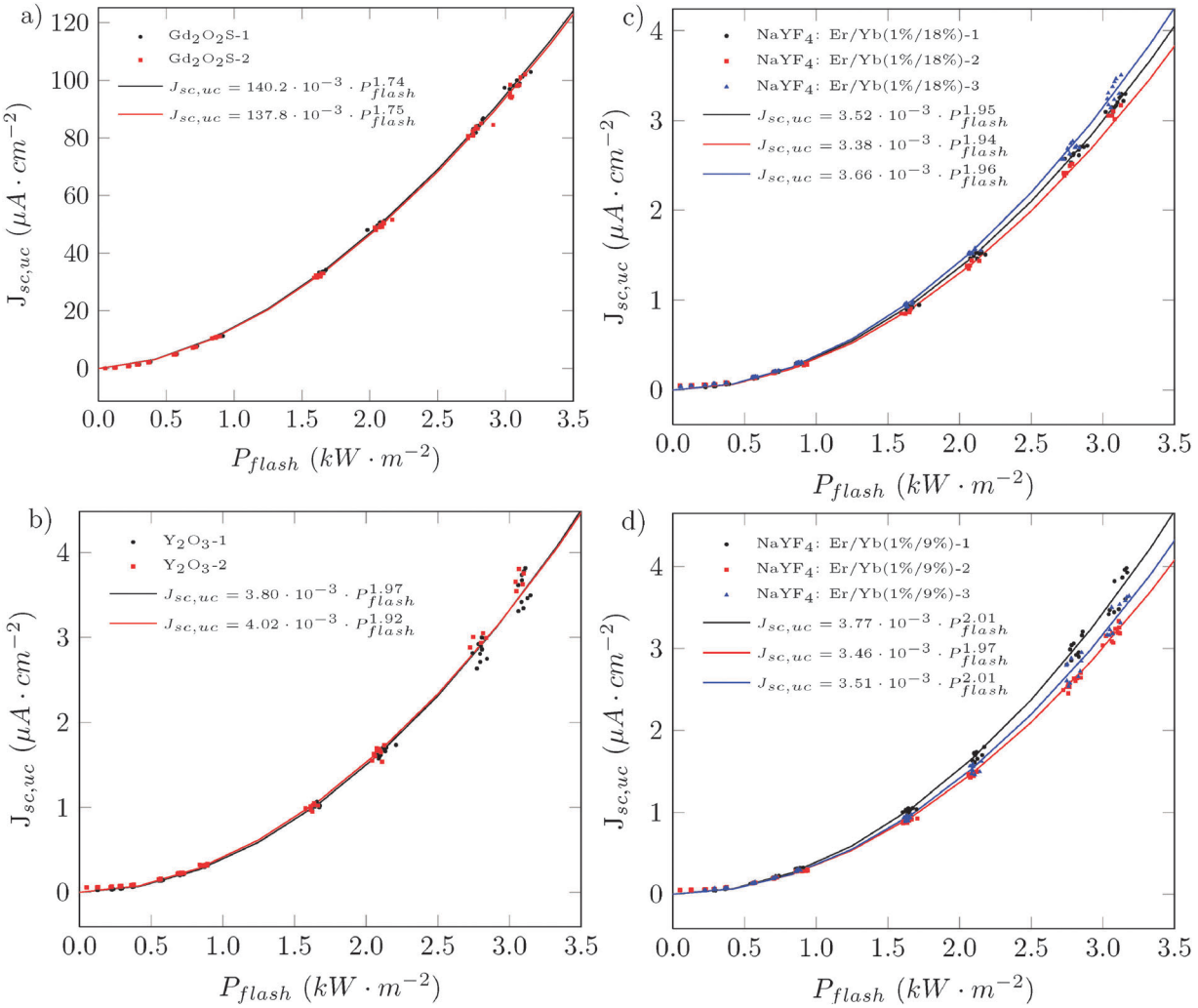

Fig. 9 Maximum upconverter induced short-circuit current density ($J_{sc,uc}$) *versus* maximum illumination power density (P_{flash}) during the same flash. Showing the InGaP solar cell in combination with Gd_2O_2S (a), Y_2O_3 (b) and $NaYF_4$ (c and d) UCS. Data points in different colors and markers represent measurements measured at 2 or 3 different days and the lines are the best least-sum-of-squares-fit with $J_{sc,uc} = aP_{flash}^{b}$ in which '*a*' and '*b*' are fit parameters.

absorption of this UCS is positioned around 950 nm which coincides with a low energy spectral range (water hole) in the AM1.5 spectrum, whereas the absorption of the $NaYF_4$ UCS is mainly located at higher wavelength than this hole. This means that $NaYF_4$ is a more suitable host material considering the wavelength range of the absorption band. Nevertheless, the absorbed power density under AM1.5 illumination is found to be higher for the Gd_2O_2S UCS case than for the $NaYF_4$ UCS. Emitted light around 550 nm is converted in the semi-transparent InGaP solar cell with a quantum efficiency of 0.5. However, the emission peaks around 660 nm are close to the cut-off wavelength of InGaP. In this region the EQE of the solar cell is rapidly decreasing. Particularly the combination of the Y_2O_3 UCS with an InGaP solar cell is not optimal for this reason, a solar cell with a higher cut-off wavelength would provide a better match.

An experimental setup was designed in which the solar cell photocurrent resulting from upconversion was measured. The solar cell and upconverter were illuminated by a xenon flash lamp producing short and intense pulses of broadband light from which all light of wavelengths below 900 nm was removed.

Table 2 Parameters of the best fit of the experimental data using eqn (6) as shown in Fig. 9. Different colors correspond with the colors in Fig. 9 from different repeated experiments. The "Average *b*" represent the combined value of *b* calculated from the individual measurements

UCS: Er^{3+}/Yb^{3+}	$a\ (10^{-4})$	b	R^2	Average b
Gd_2O_2S: 5%/10%	140.2 ± 0.9	1.739 ± 0.006	0.9996	1.742 ± 0.003
	137.8 ± 1.1	1.745 ± 0.008	0.9995	
Y_2O_3: 5%/10%	3.80 ± 0.09	1.971 ± 0.022	0.9966	1.946 ± 0.026
	4.02 ± 0.11	1.92 ± 0.03	0.9952	
$NaYF_4$: 1%/9%	3.77 ± 0.09	2.008 ± 0.022	0.9974	1.992 ± 0.025
	3.46 ± 0.05	1.967 ± 0.014	0.9988	
	3.51 ± 0.08	2.001 ± 0.022	0.9974	
$NaYF_4$: 1%/18%	3.52 ± 0.04	1.948 ± 0.010	0.9994	1.946 ± 0.011
	3.38 ± 0.06	1.935 ± 0.019	0.9977	
	3.66 ± 0.06	1.956 ± 0.015	0.9985	

Without upconverter, the measured short circuit current was zero, whereas a distinct photocurrent was measured in the presence of each upconverter. The total power density of the flash light from 900 nm to 1050 nm accumulated to 2.7 kW m^{-2}. At this power density, the maximal short circuit current density of the solar cell during a flash was 0.10 mA cm^{-2} for the Gd_2O_2S upconverter and around 0.0035 mA cm^{-2} for the other three UCS. Furthermore, a time delay was observed between the moment that the flash intensity reaches its maximum and the solar cell gives the maximum upconverter induced photocurrent, which is a typical feature of energy transfer upconversion. Another characteristic is the quadratic dependence of the emission on the absorbed light power, which is valid up to a certain illumination power density. A nearly quadratic dependence was observed for the Y_2O_3 UCS and $NaYF_4$ UCS, whereas the Gd_2O_2S UCS already showed signs of saturation.

The enhancement of InGaP solar cell short circuit current resulting from upconversion was determined to be about 0.02% under illumination of 46 suns for the Gd_2O_2S UCS and 0.001% under illumination of 36 suns for the other three UCS. The small increments in output power measured in the present study are too small to measure during regular operation of the solar cell. Therefore the approach in which all light below 900 nm was excluded from reaching the solar cell was used. Clearly the enhancement of solar cell efficiency achieved by application of an upconverter systems in the present state of development is far too low for practical applications.

Acknowledgements

We acknowledge the Institute of Molecules and Materials for the research opportunities; Utrecht University for samples and support; G. Bauhuis for InGaP solar cell fabrication and P. Mulder for InGaP solar cell processing including the ELO process.

Notes and references

1 W. Shockley and H. J. Queisser, *J. Appl. Phys.*, 1961, **32**, 510–519.
2 W. G. J. H. M. van Sark, A. Meijerink and R. E. I. Schropp, *CIER-E-2012-8*, 2012, vol. 8, pp. 1–28.
3 J. de Wild, A. Meijerink, J. K. Rath, W. G. J. H. M. van Sark and R. E. I. Schropp, *Energy Environ. Sci.*, 2011, **4**, 4835–4848.
4 B. M. van der Ende, L. Aarts and A. Meijerink, *Phys. Chem. Chem. Phys.*, 2009, **11**, 11081–11095.
5 C. Strümpel, M. McCann, G. Beaucarne, V. Arkhipov, A. Slaoui, V. Švrček, C. del Cañizo and I. Tobias, *Sol. Energy Mater. Sol. Cells*, 2007, **91**, 238–249.
6 J. F. Suyver, A. Aebischer, D. Biner, P. Gerner, J. Grimm, S. Heer, K. W. Krämer, C. Reinhard and H. U. Güdel, *Opt. Mater.*, 2005, **27**, 1111–1130.
7 A. Shalav, B. S. Richards and M. A. Green, *Sol. Energy Mater. Sol. Cells*, 2007, **91**, 829–842.
8 K. Zhang, F. Song, J. Su, L. Han, J. Liang, X. Zhang, L. Yan, J. Tian and J. Xu, *Opt. Express*, 2006, **14**, 12584–12589.
9 F. Lahoz, C. Perez-Rodriguez, S. E. Hernandez, I. R. Martin, V. Lavin and U. R. Rodriguez-Mendoza, *Sol. Energy Mater. Sol. Cells*, 2011, **95**, 1671–1677.
10 G. Chen, T. Y. Ohulchanskyy, A. Kachynski, H. Agren and P. N. Prasad, *ACS Nano*, 2011, **5**, 4981–4986.
11 F. Auzel, *et al.*, *Chem. Rev.*, 2004, **104**, 139–174.
12 F. Auzel, *et al.*, *J. Lumin.*, 1990, **45**, 341–345.
13 V. D. Rodríguez, J. Méndez-Ramos, V. K. Tikhomirov, J. del Castillo, A. C. Yanes and V. V. Moshchalkov, *Opt. Mater.*, 2011, **34**, 179–182.
14 J. de Wild, T. F. Duindam, J. K. Rath, A. Meijerink, W. G. J. H. M. Sark and R. E. I. Schropp, *IEEE J. Photovolt.*, 2012, **3**, 17–21.
15 J. De Wild, J. K. Rath, A. Meijerink, W. Van Sark and R. E. I. Schropp, *Sol. Energy Mater. Sol. Cells*, 2010, **94**, 2395–2398.
16 J. De Wild, A. Meijerink, J. K. Rath, W. Van Sark and R. E. I. Schropp, *Sol. Energy Mater. Sol. Cells*, 2010, **94**, 1919–1922.
17 P. Gibart, F. Auzel, J. C. Guillaume and K. Zahramank, *Jpn. J. Appl. Phys.*, 1996, **35**, 4401–4402.
18 J. J. Schermer, P. Mulder, G. J. Bauhuis, M. M. A. J. Voncken, J. van Deelen, E. Haverkamp and P. K. Larsen, *Phys. Status Solidi A*, 2005, **202**, 501–508.
19 H. Wang, M. Batentschuk, A. Osvet, L. Pinna and C. J. Brabec, *Adv. Mater.*, 2011, **23**, 2675–2680.
20 B. Henke, F. Pientka, J. A. Johnson, B. Ahrens, P. T. Miclea and S. Schweizer, *J. Phys.: Condens. Matter*, 2010, **22**, 155107.
21 M. Pollnau, D. R. Gamelin, S. R. Lüthi, M. P. Hehlen and H. U. Güdel, *Phys. Rev. B: Condens. Matter Mater. Phys.*, 2000, **61**, 3337–3346.
22 Y. Y. Cheng, B. Fueckel, R. W. MacQueen, T. Khoury, R. G. R. C. Clady, T. F. Schulze, N. Ekins-Daukes, M. J. Crossley, B. Stannowski and K. Lips, *Energy Environ. Sci.*, 2012, **5**, 6953.
23 T. N. Singh-Rachford and F. N. Castellano, *J. Phys. Chem. A*, 2009, **113**, 5912–5917.
24 J. F. Suyver, J. Grimm, M. K. van Veen, D. Biner, K. W. Kramer and H. U. Gudel, *J. Lumin.*, 2006, **117**, 1–12.
25 T. Trupke, M. A. Green and P. Wurfel, *J. Appl. Phys.*, 2002, **92**, 4117–4122.
26 A. C. Atre and J. A. Dionne, *J. Appl. Phys.*, 2011, **110**, 034505.
27 S. Ivanova and F. Pell, *J. Opt. Soc. Am. B*, 2009, **26**, 1930–1938.
28 G. Blasse and B. C. Grabmaier, *Luminescent materials*, Springer-Verlag, Berlin, 1994, vol. 44, ISBN: 978-3-642-79017-1.
29 M. A. Green, K. Emery, Y. Hishikawa, W. Warta and E. D. Dunlop, *Prog. Photovoltaics*, 2012, **20**, 606–614.
30 http://scidavis.sourceforge.net/contributing.html visited on: 01-05-2014.
31 J. J. Schermer, G. J. Bauhuis, P. Mulder, E. J. Haverkamp, J. van Deelen, A. T. J. van Niftrik and P. K. Larsen, *Thin Solid Films*, 2006, **511–512**, 645–653.